CROSS FEEDBACK CONTROL OF A MAGNETIC BEARING SYSTEM
Controller Design Considering Gyroscopic Effects

Markus Ahrens
International Center for Magnetic Bearings, ETH Zurich
Switzerland

Ladislav Kučera
International Center for Magnetic Bearings, ETH Zurich
Switzerland

ABSTRACT

For flywheel rotors or other rotors with significant ratios of moments of inertia ($J_z/J_x \not\ll 1$, see figure 2), the influence of gyroscopic effects has to be considered. While conservative or damped systems remain stable even under gyroscopic effects, magnetically suspended rotors can be destabilized with increasing rotational speed.

The influence of gyroscopic effects on the stability and behaviour of a magnetic bearing system is analyzed. The analysis is carried out with a rigid body model for the rotor and a nonlinear model for the magnetic bearing and its amplifier.

Cross feedback control can compensate gyroscopic effects. This compensation leads to better system performance and can avoid instability. Furthermore, the implementation of this compensation is simple. The main structure of a decentralized controller can still be used. It has only to be expanded by the cross feedback path.

INTRODUCTION

Magnetic bearings are used in a wide field of applications due to their advantages compared to other bearing types. The main advantages are that they operate contact free, they have low friction losses, adjustable damping and stiffness characteristics and the fact that no lubricants are necessary. They are therefore ideally suited for high speed and vacuum applications.

A magnetic bearing system is unstable in nature and therefore a controller is required. In order to design a controller a mathematical model of the plant is necessary.

The rotor can be described as a $MDGK$-system (see equation 8). The gyroscopic matrix G describes the coupling between the rotor axes while rotating.

For rotors with a small ratio of moments of inertia ($J_z/J_x \ll 1$) the gyroscopic coupling is small and can be neglected. In this case the system can be divided into two identical subsystems (x-z and y-z plane) which can be controlled independently. For many magnetic bearing systems, decentralized controllers are used which control each bearing unit independently. In [Ble84] it is shown that gyroscopic systems can be controlled with decentralized controllers.

In [Mag71] and [MS76] it is shown that conservative stable systems cannot become unstable

177

with gyroscopic effects. Magnetically suspended rotors however, cannot usually be considered as conservative. There are mainly two reasons that stability cannot be guaranteed for magnetic bearing systems. In [Her91] it is shown that the plant is no longer positive-real, when digital controllers are used. In [ME93] it is shown that gyroscopic effects can cause instability when certain nonlinearities are considered.

For rotors with a ratio of moments of inertia which is not small ($J_z/J_x \not\ll 1$) (e.g. pumps, turbines and especially flywheels) or rotors with extremely high rotational speeds, the influence of gyroscopic effects has to be considered. In [MH84] it can be seen that centralized control (using LQR) considering gyroscopic effects can achieve better system performance than decentralized control. This is only valid however for the specified rotational speed. In [Ulb79] it is shown that a controller designed with LQR at a certain rotational speed can lead to instability at standstill. In [ONS89] cross feedback control is proposed. Here, the controller has a cross coupling which is displacement-proportional and can avoid instability of the precession mode.

In 1992 a project was started at the ETH Zurich[1] to develop a flywheel energy storage device using magnetic bearings. The following analysis was made within the scope of this project.

MODEL

This chapter describes the model structure used for the theoretical analysis of gyroscopic effects. The model structure is as extensive as necessary to solve the desired problems.

The authors used MAPLE [Hec93] for an analytical model, MATLAB [GLLT92] for linear modelling, controller design and transfer functions and ACSL [Mit93] for nonlinear simulations.

Magnetic Bearing

This section defines the nonlinear force and voltage equations of the electromagnets. The model will include the resistance of the coil R and the leakage inductance L_s. All other effects are neglected. All magnets (planes a and b, directions x and y, sides 1 and 2) have identical structures. The following equations are given for the magnets 1 and 2 of plane a and direction x. The equations for the other magnets are analogous.

Steady state definitions:

$x_{a1,2}$: air gap between electromagnet 1 (respectively 2) and the rotor.
x_0 : steady state air gap.
x_a : deviation from the steady state position.

$i_{xa1,2}$: current through the coil of electromagnet 1 (respectively 2).
i_0 : bias current.
i_{xa} : control current.

$F_{xa1,2}$: force of electromagnet 1 (respectively 2) acting on the rotor.
F_{xa} : total force acting on the rotor (including the disturbance force $F_{s,xa}$).

$u_{xa1,2}$: voltage across the coil of electromagnet 1 (respectively 2).
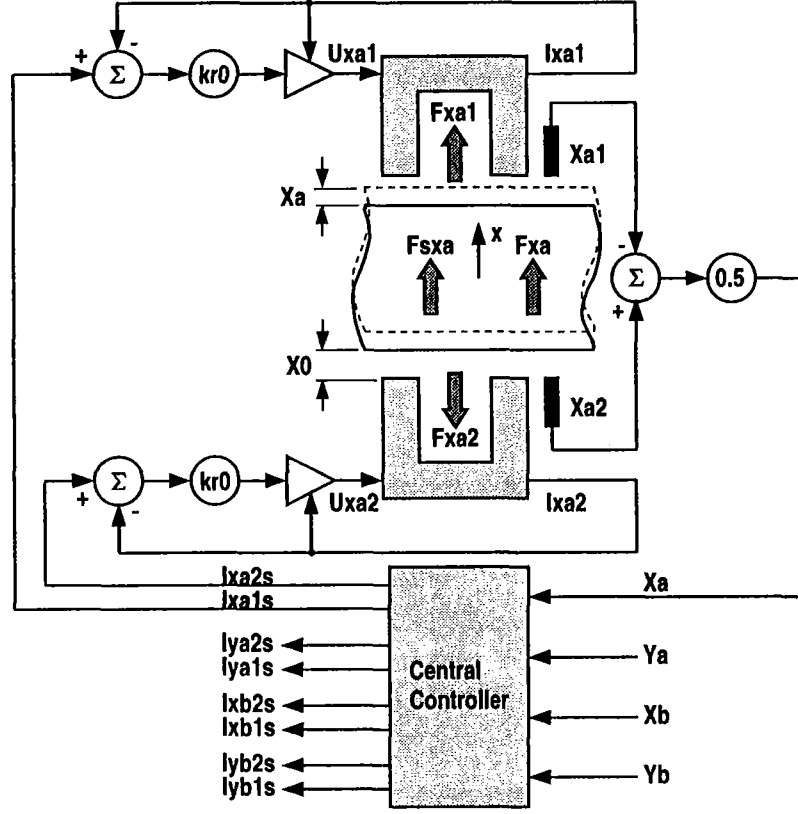
Figure 1: Definitions of the magnetic bearing model.

$$x_{a1} = x_0 - x_a, \qquad x_{a2} = x_0 + x_a \tag{1}$$

$$i_{xa1} = i_0 + i_{xa}, \qquad i_{xa2} = i_0 - i_{xa} \tag{2}$$

$$F_{xa1} = \frac{K}{4}\frac{i_{xa1}^2}{x_{a1}^2}, \qquad F_{xa2} = \frac{K}{4}\frac{i_{xa2}^2}{x_{a2}^2} \tag{3}$$

and

$$F_{xa} = F_{xa1} - F_{xa2} + F_{s,xa} \tag{4}$$

The constant $K = \mu_0 N^2 A$ represents electrical and geometrical characteristics of an electromagnet. $\mu_0 = 4\pi 10^{-7}\,(\text{Vs})/(\text{Am})$, N is the number of turns of the coil and A the area of one magnetic pole.

The linearized force equation with $k_s = \frac{K}{2}\frac{i_0^2}{x_0^3}$ and $k_i = \frac{K}{2}\frac{i_0}{x_0^2}$ is given by:

$$F_{xa} = 2k_s x_a + 2k_i i_{xa} + F_{s,xa} \tag{5}$$

179

The voltage across the coil of an electromagnet can be considered to be derived from an electrical effect which does not depend on x_a and is dependent upon R and L_s, and a second electromechanical effect which depends on x_a:

$$u_{xa1} = Ri_{xa1} + L_s\frac{di_{xa1}}{dt} + \frac{K}{2}\frac{i_{xa1}}{x_{a1}}, \qquad u_{xa2} = Ri_{xa2} + L_s\frac{di_{xa2}}{dt} + \frac{K}{2}\frac{i_{xa2}}{x_{a2}} \tag{6}$$

Rotor

In the following calculations a rigid body model is used. The equations of motion for a rotor can be described in body coordinates $\bar{q}$.

The equation of motion for the z-direction is independent of the equations of motion for the x- and y-direction. In the following analysis, the motion in the z-direction is neglected, because it is independent of gyroscopic effects.
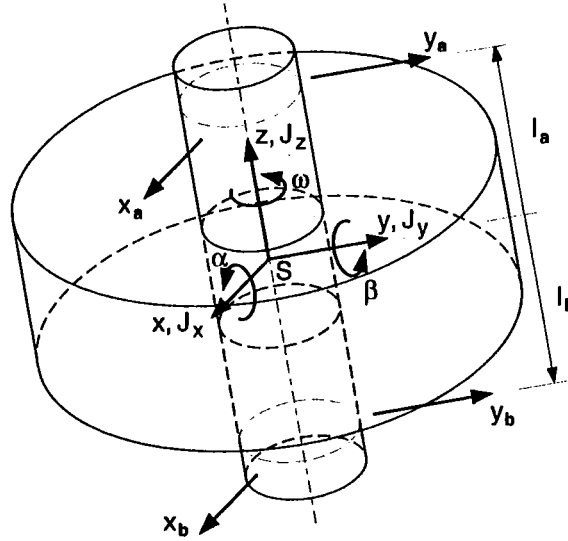

Figure 2: Definition of the moments of inertia and geometry definitions of the rigid body model, body coordinates $\bar{q}$ and bearing coordinates q. S defines the centre of gravity.

$$\bar{q} = \begin{pmatrix} \beta \\ x \\ -\alpha \\ y \end{pmatrix} \tag{7}$$

The equations of motion can be written as:

$$M\ddot{\bar{q}} + (D + \omega G)\dot{\bar{q}} + K\bar{q} = F \tag{8}$$

In equation (8), M is the symmetric mass matrix, D the symmetric damping matrix, G the skew-symmetric gyroscopic matrix, K the symmetric stiffness matrix and F the bearing forces. For the rigid body model the matrices are:

$$M = \begin{pmatrix} J_x & 0 & 0 & 0 \\ 0 & m & 0 & 0 \\ 0 & 0 & J_x & 0 \\ 0 & 0 & 0 & m \end{pmatrix} \qquad (9)$$

$$D = 0 \qquad (10)$$

$$G = \begin{pmatrix} 0 & 0 & J_z & 0 \\ 0 & 0 & 0 & 0 \\ -J_z & 0 & 0 & 0 \\ 0 & 0 & 0 & 0 \end{pmatrix} \qquad (11)$$

$$K = 0 \qquad (12)$$

$$F = B_z f \qquad (13)$$

$$B_z = \begin{pmatrix} l_a & l_b & 0 & 0 \\ 1 & 1 & 0 & 0 \\ 0 & 0 & l_a & l_b \\ 0 & 0 & 1 & 1 \end{pmatrix} \qquad (14)$$

$$f = \begin{pmatrix} F_{xa} \\ F_{xb} \\ F_{ya} \\ F_{yb} \end{pmatrix} \qquad (15)$$

A transformation to bearing coordinates q leads to the following equations. The bearing coordinates are:

$$q = \begin{pmatrix} x_a \\ x_b \\ y_a \\ y_b \end{pmatrix} \qquad (16)$$

The transformation can be written as:

$$q = T\bar{q} \qquad (17)$$

where T is the transformation matrix:

$$T = \begin{pmatrix} l_a & 1 & 0 & 0 \\ l_b & 1 & 0 & 0 \\ 0 & 0 & l_a & 1 \\ 0 & 0 & l_b & 1 \end{pmatrix} \qquad (18)$$

The transformed equations of motions are:

$$\ddot{q} = -TM^{-1}\omega GT^{-1}\dot{q} + TM^{-1}B_z f \qquad (19)$$

When a linearized bearing model is used, f can be written as:

$$f = K_s q + K_i i \qquad (20)$$

In equation (20), K_s is the force-displacement factor and K_i the force-current factor.

$$K_s = \begin{pmatrix} 2k_{s,a} & 0 & 0 & 0 \\ 0 & 2k_{s,b} & 0 & 0 \\ 0 & 0 & 2k_{s,a} & 0 \\ 0 & 0 & 0 & 2k_{s,b} \end{pmatrix} \qquad (21)$$

$$K_i = \begin{pmatrix} 2k_{i,a} & 0 & 0 & 0 \\ 0 & 2k_{i,b} & 0 & 0 \\ 0 & 0 & 2k_{i,a} & 0 \\ 0 & 0 & 0 & 2k_{i,b} \end{pmatrix} \qquad (22)$$

In this case K_s leads to a non-zero stiffness matrix K.

For all further analysis, the location of the sensors is assumed to be identical with the location of the corresponding bearing forces (collocation).

Amplifier

The output voltage amplitude of an amplifier is limited to a lower and an upper boundary (u_{min} and u_{max}). The output current cannot exceed a maximal value i_{max} or become negative (in a two quadrant amplifier).
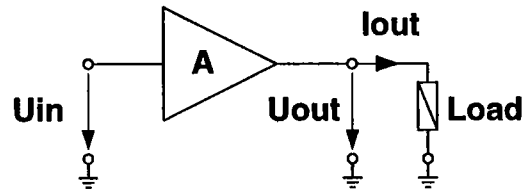

Figure 3: Diagram of the amplifier

$$u_{out} = \begin{cases} u_{max} & : & u_{in} \geq u_{max} \\ u_{in} & : & u_{min} < u_{in} < u_{max} \\ u_{min} & : & u_{in} \leq u_{min} \end{cases} \qquad (23)$$

and

$$0 \leq i_{out} \leq i_{max} \qquad (24)$$

Voltage saturation of an amplifier leads to reduced dynamics of the current. This is shown in figure 4 and 5 for an example. Current bandwidth can be approximated by a low pass of first order with variable cut-off frequency (depending on the magnitude of the current bouncing). A current controller has a fixed cut-off frequency which can be adjusted with the feedback gain kr_0 (see figure 4).
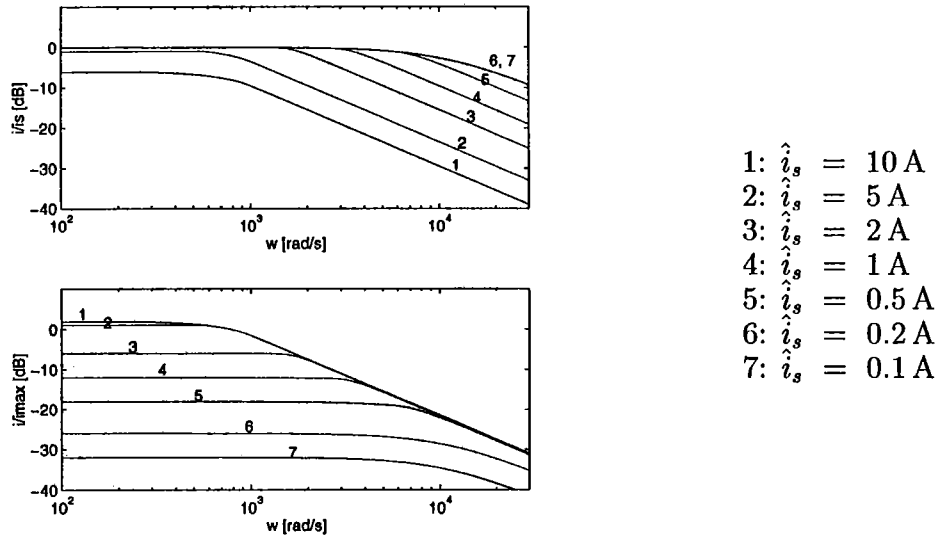

1: $\hat{i}_s$ = 10 A
2: $\hat{i}_s$ = 5 A
3: $\hat{i}_s$ = 2 A
4: $\hat{i}_s$ = 1 A
5: $\hat{i}_s$ = 0.5 A
6: $\hat{i}_s$ = 0.2 A
7: $\hat{i}_s$ = 0.1 A

Figure 4: Dynamics of a current controller with saturated amplifier. The upper plot shows the transfer function $|G_1(j\omega)| = |\frac{i(j\omega)}{i_s(j\omega)}|$ and the lower plot the transfer function $|G_2(j\omega)| = |\frac{i(j\omega)}{i_{max}}|$ normalized to maximum current. $|G_2(j\omega)|_{max} = \frac{4}{\pi}$ and not 1 (the first spectral fourier coefficient of a periodic square wave).
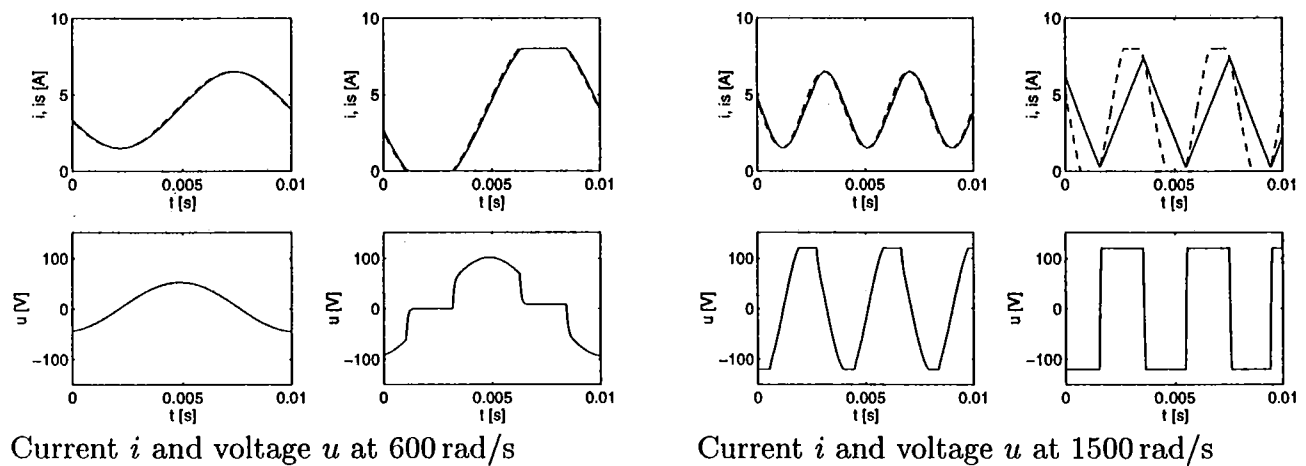

Current i and voltage u at 600 rad/s

Current i and voltage u at 1500 rad/s

Figure 5: Current i and voltage u at two frequencies.
i_s is the desired current and is plotted with dashed line. In the left hand plots $\hat{i}_s$ = 2.5 A and in the right hand plots $\hat{i}_s$ = 5 A. The saturation current i_{max} = 4 A.

The function of a digital controller can be divided into an input signal processing block, a controller and an output signal processing block. The following diagrams show the model structure of a state space current controller. Observers for all velocities of the rotor are part of the input block.

The input block models an AD-converter with quantized and sampled output. The derivation of the input signal is made by shifting the input signal N time steps and performing a backward integration (see figure 25). The purpose of the shifting factor N is to enlarge the resolution of the velocity signal at high sampling frequencies.

$$\dot{x}_{aq} = \frac{z^N - 1}{z^N T_s N} x_a \qquad (25)$$

The output block models a DA-converter with a quantized and delayed output. The delay is caused by the calculation time of the processor.
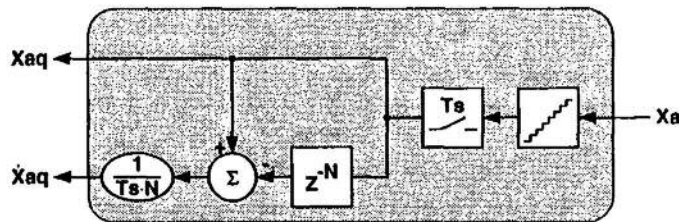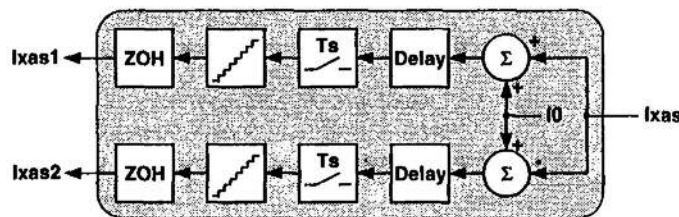

Figure 6: Input signal processing.

Figure 7: Output signal processing.

BEHAVIOUR OF MAGNETICALLY SUSPENDED GYROSCOPES

In this section, the basic behaviour of gyroscopes with magnetic suspension is shown. More information on the behaviour of gyroscopes in general can be found in [Mag71].

At first, system behaviour is shown for a linearized bearing model (refer to equation 20) using a decentralized PD-controller. In this case the rotor behaves like an elastically suspended gyroscope (suspension with a spring and damper). This is a damped mechanical system ($M = M^T > 0, K = K^T > 0, D = D^T > 0$) and, therefore, stable ([Mag71],[MS76]).
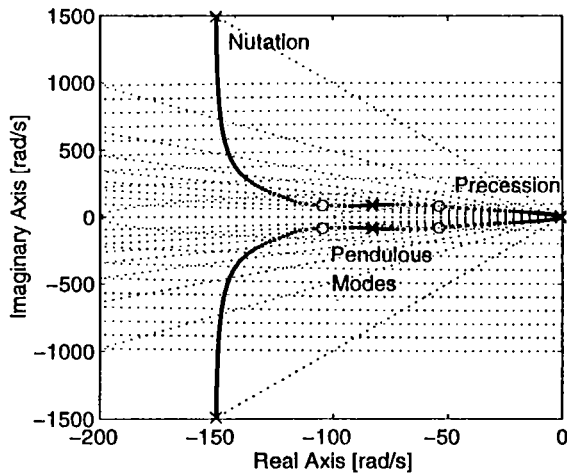
184

Figure 8: Poles of the system depending on the rotational speed, $\omega = 0 \ldots 1250\,\text{rad/s}$,
o: poles at $\omega = 0\,\text{rad/s}$,
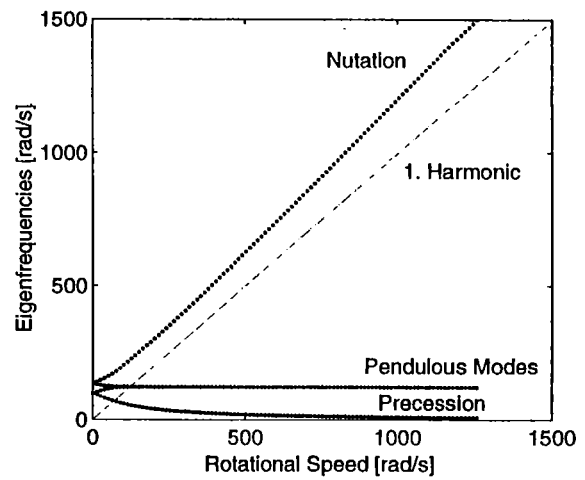×: poles at $\omega = 1250\,\text{rad/s}$

Figure 9: Campbell diagram of the rigid body model,
$\omega = 0 \ldots 1250\,\text{rad/s}$,

The non-rotating system has two eigenfrequencies which are equal for the x-z plane and the y-z plane. For the rotating rotor these eigenfrequencies become coupled and depend on the rotational speed. The four eigenfrequencies are a nutation, two pendulous and a precession frequency. The nutation frequency increases with the rotational speed ($\lim_{\omega \to \infty} \omega_N = \omega \frac{I_z}{I_x}$), while the precession frequency decreases ($\lim_{\omega \to \infty} \omega_P = 0$) [Mag71], [SBT94].
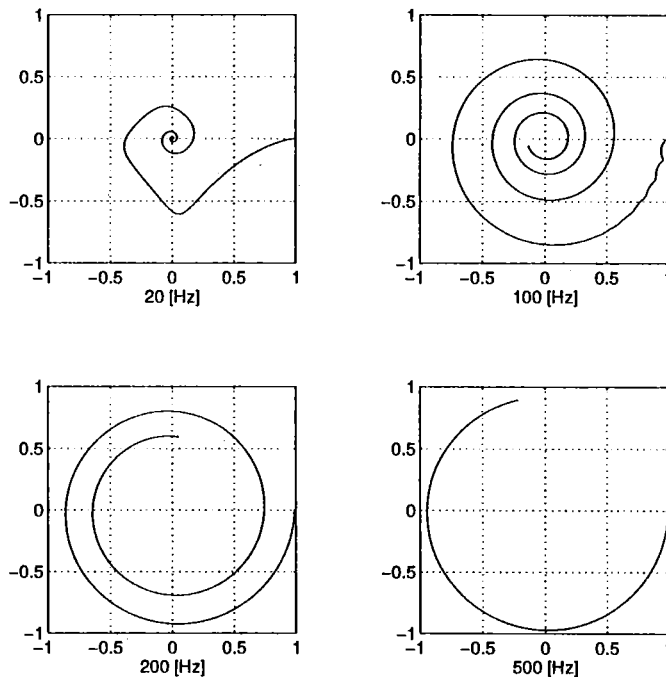

Figure 10: Response of the rotor in the upper plane due to an angular displacement ($\Delta x_a = -\Delta x_b$), The recording time was 1s for all plots, $\omega = 20\,\text{Hz}$, $100\,\text{Hz}$, $200\,\text{Hz}$ and $500\,\text{Hz}$

It is assumed that all states (positions and velocities) can be measured or observed. Then the following feedback law can be used:

$$u = -K_r x \qquad (26)$$

In equation (26) u is the control input vector, x the state vector and K_r the feedback matrix.
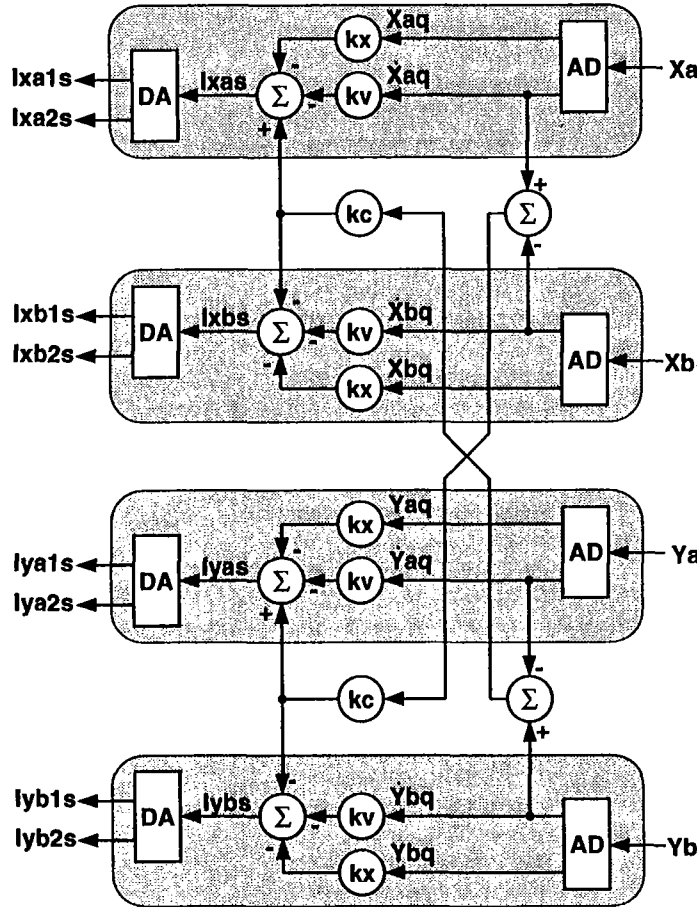

Figure 11: Decentralized controller with compensation of the gyroscopic cross coupling.

For many magnetic bearing systems, decentralized control is used. In that case, each magnetic bearing unit is a subsystem which is controlled independently [Ble84]. The feedback matrix K_r therefore only consists of diagonal elements. There is no cross coupling between the x- and y-direction and respectively the two radial bearing planes. The main advantages of decentralized control are simple controller structure and reduced computational time. For a system at standstill, and respectively for a system with weak gyroscopic coupling, decentralized control leads to good system performance which cannot be significantly improved with centralized control. In the case of a magnetic bearing system with strong gyroscopic coupling, the situation is different. The plant changes with the rotational speed. As mentioned before,

186

gyroscopic coupling leads to a decrease of system performance because the precession mode becomes limit stable. A consideration of digitization and other nonlinearities (see next section) shows that gyroscopic effects can cause instability. Therefore, gyroscopic coupling has to be considered for controller design.

A centralized controller can be designed at a certain rotational speed so that the system has the same poles as at standstill. In this case gyroscopic effects are compensated. This compensation leads to additional terms in the feedback matrix K_r which depend on rotor velocities and are proportional to the rotational speed. Furthermore, these additional terms only occur outside the diagonals of K_r. A decentralized controller designed to operate at standstill therefore remains unaffected by this compensation. Figure 11 shows a simple realisation of a decentralized controller expanded with a compensation of the gyroscopic cross coupling.

The compensation factor k_c is:

$$k_c = \frac{C_{att}\omega J_z}{k_i(l_a - l_b)^2} \tag{27}$$

Further analysis shows that a system with complete compensation of gyroscopic effects is not robust to a delay time (see next section). An attenuation factor C_{att} is used to improve robustness. The structure of the compensator remains the same.

Figure 12 shows the behaviour of a rotor at a rotational speed of 1000 rad/s with a decentralized controller. The increase of system performance with cross feedback can be clearly seen (figure 13).
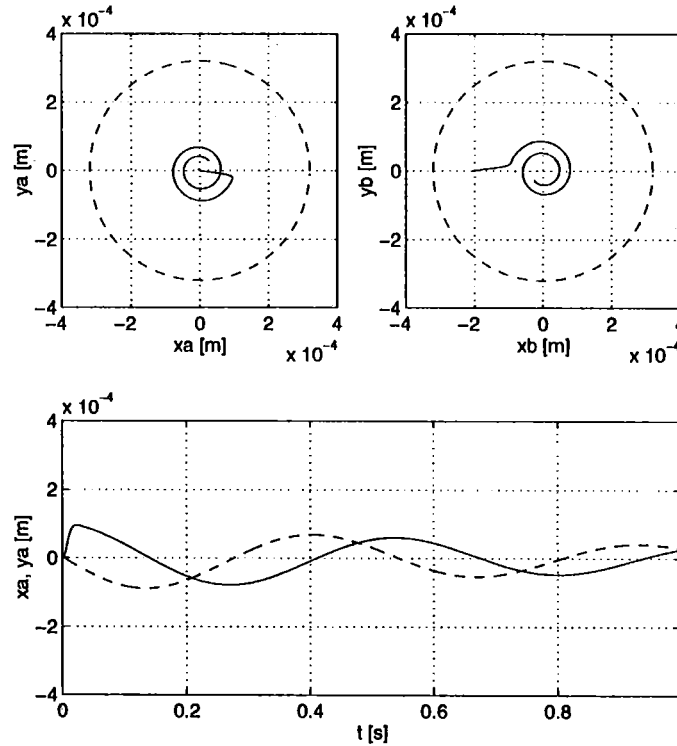

Figure 12: Decentralized controller and transient motion of the excited rotor (dashed line: retainer bearing), $\omega = 1000$ rad/s
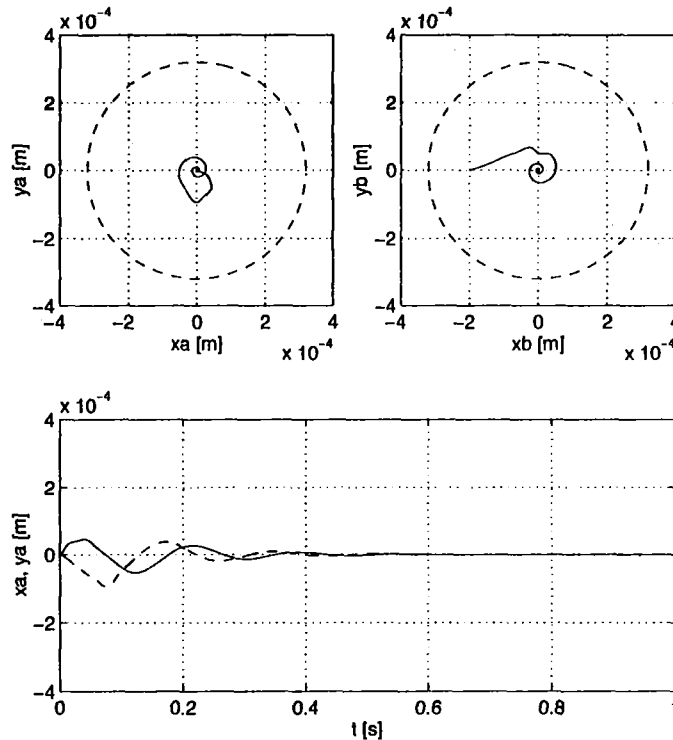
187

Figure 13: Decentralized controller with 70% compensation of the gyroscopic coupling and transient motion of the excited rotor (dashed line: retainer bearing), $\omega = 1000$ rad/s

It should be noted, that the expansion is small and, therefore, computation time will not increase much. Compared to a full centralized feedback matrix, computation time is nearly four times less. Furthermore, the implementation of this compensation is simple. The main structure of the decentralized controller can still be used. It only has to be expanded by the cross feedback path.

NONLINEARITIES AND SYSTEM PERFORMANCE

As mentioned before, a conservative or damped system cannot be destabilized by gyroscopic effects. A passive (positive-real) continous time controller would therefore be sufficient for stability. In [Her91] it is pointed out that the plant is no longer positive-real when digital controllers are used. Stability cannot therefore be guaranteed for a real nonlinear magnetic bearing with a digital controller.

Sampling Time

The choice of the sampling rate depends on the control of the fastest pole of the closed-loop system. The lowest sampling rate is given by Shannon's law and must be 2 times faster (in practice 5 ... 10 times) than the fastest closed-loop pole.

188

Typically the open-loop poles of a plant are slower than the closed-loop poles. The system "rotating rotor with gyroscopic coupling", however, behaves differently. At high rotational speed, the fastest open-loop pole can become faster than the closed-loop poles.
Sampling of a digital controller can be modelled with a ZOH (zero order hold) element. The transfer function is:

$$G_{zoh}(s) = \frac{1 - e^{sT_{samp}}}{s} \quad ; \quad G_{zoh}(j\omega) = \frac{1 - e^{-j\omega T_{samp}}}{j\omega} = \frac{2\sin(\frac{\omega T_{samp}}{2})}{\omega}e^{-j\frac{\omega T_{samp}}{2}} \quad (28)$$

It can be seen in equation (28) that a ZOH element introduces a phase shift of $\frac{\omega T_{samp}}{2}$. At the sampling frequency $f_{samp} = 1/T_{samp}$ the phase shift is $-180°$. Therefore, the stability margin for the nutation mode decreases. When the open-loop phase is under $-180°$ due to the phase shift caused by digitization, delay time, etc., instability can occur for the nutation mode (open-loop gain > 1).

The delay time is normally caused by computational time. Similarly to the sampling time, the delay time can be represented as a linear phase shift. This additional phase shifting leads to further reduction of the stability margin.

Current Controller and Amplifier Saturation

The dynamics of a current controller should be as fast as possible. Current controllers with slow dynamics have a phase shift of $-90°$ at the cut-off frequency. This phase shift leads to the same instability problems as mentioned before.
Saturation of the amplifier, i.e. limitation of voltage, leads to a delayed start of the current and, therefore, to an additional phase shift.
Current limitation mainly decreases the magnitude. The phase is unaffected (see also [Unb93b]) and, therefore, instability problems do not occur. A nonlinear simulation shows that the rotor is stable even with high current saturation (see figure 14).
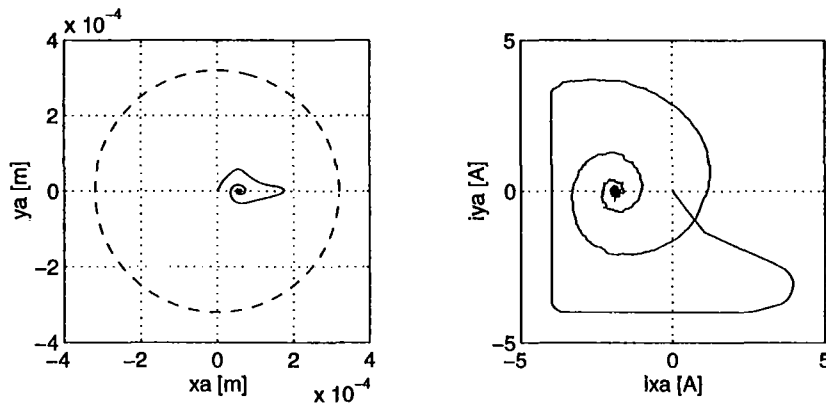

Figure 14: Transient motion of the rotor with an external disturbance force (dashed line: retainer bearing). The current is limited to 4 A.

Robustness of the Compensation

Nonlinearities such as digitization, delay time and amplifier saturation which lead to a delayed reaction of a compensator can cause instability of the system. The smaller these delays are, the better the compensation will work.

For systems with strong gyroscopic coupling, a controller with compensation has to be proposed to improve system performance. Complete compensation has been shown to be possible in linear simulations with MATLAB, but still leads to instability in practice. Nonlinear simulations (with ACSL) show that complete compensation is not robust to delay time effects. An attenuation factor C_{att} is therefore used. It gives the ratio of the implemented compensation compared to a complete compensation. The structure of the cross coupling remains the same, but robustness is much higher. A sufficient and robust solution can be found with an attenuation factor of 75%. With complete compensation, the system has the same behaviour as at standstill. With reduced compensation (e.g. 75%) the system behaviour is the same as for a reduced rotational speed (25% of the nominal rotational speed).

In this paper cross feedback control is analyzed for current control and voltage control with a fast current controller. Here, the rotor poles are independent of the poles of the current controller. For voltage control with a slow current controller, the relationship between the coefficients and the rotational speed is not obvious. In this case all system poles including the poles of the current controller depend on the rotational speed. Further analysis is therefore necessary for voltage controlled systems.

Simulations show that current errors caused by a current observer can easily cause instability. Current observers should therefore not be used for systems with a compensation of gyroscopic effects.

Nonlinear Force Characteristics

The nonlinear force characteristics of magnetic bearings is not crucial for an analysis of gyroscopic effects. Simulations show that this nonlinearity is negligible in the air gap region due to the differential setup of the magnets and the use of a bias current.

CONCLUSIONS

A theoretical analysis has shown that, for rotors with strong gyroscopic coupling, all nonlinearities which decrease the phase (digital control, delay time, slow current controller) can lead to instability at very high rotational speed.

The proposed compensation improves the transient behaviour of the rotor and, therefore, system performace. It can avoid the precession mode to become limit stable. The implementation of this compensation is simple. The structure of a decentralized control can still be used.

With analogue control which introduces no phase shift, stability problems can be reduced. The flexibility of digital control has however certain advantages (e.g. unbalance compensation).

In the next step, these theoretical results will be tested on the flywheel energy storage device.

REFERENCES

[Ack88] Jürgen Ackermann. *Abtastregelung*. Springer-Verlag, Berlin, 1988.

[Ble84] Hannes Bleuler. *Decentralized Control of Magnetic Rotor Bearing Systems*. PhD thesis, ETH Swiss Federal Institute of Technology, Zurich, 1984.

[GLLT92] Grace, Laub, Little, and Thompson. *MATLAB Control System Toolbox, User's Guide*. Natick, 1992.

[Hec93] Andre Heck. *Introduction to Maple*. Springer-Verlag, Berlin, 1993.

[Her91] Raoul Herzog. *Ein Beitrag zur Regelung von magnetgelagerten Systemen mittels positiv reeller Funktionen und $\mathcal{H}^\infty$-Optimierung*. PhD thesis, ETH Eidgenössische Technische Hochschule, Zürich, 1991.

[Mag71] Kurt Magnus. *Kreisel, Theorie und Anwendungen*. Springer-Verlag, Berlin, 1971.

[ME93]   A.M. Mohamed and F.P. Emad. Nonlinear Oscillations in Magnetic Bearing Systems. *Transactions on Automatic Control*, 38, August 1993.

[MH84]   Takeshi Mizuno and Toshiro Higuchi. Design of the Control System of Totally Active Magnetic Bearings. In *International Symposium on Design and Synthesis*, Tokyo, 1984.

[Mit93] Mitchell and Gauthier, Concord. *ACSL Reference Manual*, 1993.

[MS76]   Peter C. Müller and Werner O. Schiehlen. *Lineare Schwingungen*. Akademische Verlagsgesellschaft, Wiesbaden, 1976.

[ONS89] Y. Okada, B. Nagai, and T. Shimane. Cross Feedback Stabilization of the Digitally Controlled Magnetic Bearing. In *Conference on Mechanical Vibration and Noise*, Montreal, 1989. ASME.

[SBT94] G. Schweitzer, H. Bleuler, and A. Traxler. *Active Magnetic Bearings*. vdf, Zurich, 1994.

[Ulb79] Heinz Ulbrich. *Entwurf und Lagerung einer berührungsfreien Magnetlagerung für ein Rotorsystem*. PhD thesis, TU München, 1979.

[Unb93a] Rolf Unbehauen. *Regelungstechnik I*. Vieweg, Braunschweig, 1993.

[Unb93b] Rolf Unbehauen. *Regelungstechnik II*. Vieweg, Braunschweig, 1993.